*International Journal of Minerals, Metallurgy and Materials*
*Volume 27, Number 11, November 2020, Page 1449*
**https://doi.org/10.1007/s12613-020-1992-5**

# Microwave-assisted reduction roasting–magnetic separation studies of two mineralogically different low-grade iron ores

*Subhnit K. Roy*[1)], *Deepak Nayak*[1)], *Nilima Dash*[1)], *Nikhil Dhawan*[2)], *and Swagat S. Rath*[1)]

1) Mineral Processing Department, CSIR-Institute of Minerals and Materials Technology, Bhubaneswar 751013, India
2) Department of Metallurgical and Materials Engineering, Indian Institute of Technology, Roorkee 247667, India
(Received: 28 September 2019; revised: 22 December 2019; accepted: 26 December 2019)

**Abstract:** The microwave-assisted reduction behaviours of two low-grade iron ores having a similar Fe content of 49wt% but distinctly different mineralogical and liberation characteristics were studied. Their performances in terms of the iron grade and recovery as obtained from statistically designed microwave (MW) roasting followed by low-intensity magnetic separation (LIMS) experiments were compared. At respective optimum conditions, the titano-magnetite ore (O1) could yield an iron concentrate of 62.57% Fe grade and 60.01% Fe recovery, while the goethitic ore (O2) could be upgraded to a concentrate of 64.4% Fe grade and 33.3% Fe recovery. Compared with the goethitic ore, the titano-magnetite ore responded better to MW heating. The characterization studies of the feed and roasted products obtained at different power and time conditions using X-ray diffraction, optical microscopy, vibrating-sample magnetometry, and electron-probe microanalysis explain the sequential reduction in the iron oxide phases. Finally, taking advantage of the MW absorbing character of the titano-magnetite ore, a blend of the same with the goethite-rich ore at a weight ratio of 60 : 40 (O2 : O1) was subjected to MW roasting that resulted in a concentrate of 61.57% Fe grade with a Fe recovery of 64.47%.

**Keywords:** microwave; reduction roasting; titano-magnetite ore; goethitic ore; magnetic separation

## 1. Introduction

The coupled approach of reduction roasting followed by magnetic separation is an effective way to recover iron values from lean-grade iron ore resources that are difficult to treat through physical beneficiation routes [1–2]. This process is not only suitable for upgrading the iron content in mineralogically complex and unliberated iron ores but also suitable for achieving a higher Fe grade and recovery compared with complicated beneficiation circuits [3–4]. With the gradual depletion of high-grade iron ores and the increasing demand for iron and steel, the research on an alternative beneficiation strategy such as reduction roasting is gaining importance nowadays [5].

Microwave (MW) heating has many advantages over conventional heating, the most prominent one being the rapid and material selective heating [6]. Conventional heating has a significant bottleneck in terms of its inability to stream the heat volumetrically, which results in a roasted mass with "cold centers". On the other hand, MW heating has an inherent property of heating the entire volume of the material [7–8]. Microwave irradiation is found to heat the interior of the material volume more than the surface [9–10]. This inverted temperature gradient can be easily observed on numerous materials, including metal oxides, which have a poor thermal conductivity [11]. Microwave-material interaction depends on many factors such as real ($\varepsilon'$) and imaginary permittivities ($\varepsilon''$), heat capacity, power level, the geometry and mass of the sample, the presence of coupling agents, and the occurrence of a chemical reaction or phase changes [12].

The application of MW energy in the carbothermal reduction roasting of low-grade iron ores can be considered as a relatively new approach. Wu *et al.* [13] investigated the phase transformation and magnetic properties of a limonitic ore having a feed of 40.1wt% Fe via MW roasting with alkali lignin as reductant and found that the goethite and hematite phases present in the ore could be successively reduced to magnetite with a grade of 57.19% Fe. Raypudi *et al.* [14] investigated the MW-assisted reduction roasting of a banded iron ore (37wt% Fe) using charcoal as the reductant. The process resulted in a magnetic concentrate of 61.6wt% Fe under conditions such as an MW power of 720 W, a charcoal dosage of 9wt%, and time of 8 min. Other than the significant advantages such as a faster reduction rate, the minimal

Corresponding author: Swagat S. Rath E-mail: ssrath@immt.res.in

formation of detrimental phases such as fayalite in the MW-roasted mass has also been reported [15]. Apart from reduction studies, the influence of MW pretreatment has also been investigated in the grindablity tests of some iron ores [16–17].

Since several ores have different MW heating behaviours, it is essential to explore the variation in the MW responses of low-grade iron ores having distinctly different mineralogical characteristics and liberation patterns; however, such investigation is yet rare in the literature. The behaviour of coal, which is not a great MW absorber, as a reductant in MW environment is also yet to be established as most of the studies reported so far have used high-pure graphite or charcoal as the carbothermic reducing agent [14–15,18]. In this context, the present work explores the MW-assisted reduction roasting of two low-grade iron ores with almost the same iron content but distinct mineralogical properties. One of them is mine overburden rich in goethite while the other one is a titano-magnetite ore.

During the process of selective mining, the majority of the low-grade hematitic ores are rejected because of their incorporation with other mineral phases such as goethite, kaolinite, and gibbsite. These phases are chemically bound with the water in the matrix, resulting in a high loss on ignition (LOI). This eventually results in high-pressure steam during the induration of the pellets, causing cracks inside the pellets, which leads to reduced strength. These overburden ores are not only fragile due to the inter-granular pore spaces and voids along the weaker bedding planes [19] but also not upgradable through physical separation processes mostly due to liberation issues [20]. The reduction roasting–magnetic separation method has been successfully implemented for such goethetic ores [21–22]. However, the response of such ores to MW-assisted carbothermic reduction roasting is yet to be established. On the other hand, the titano-magnetite ores contain ilmenite and magnetite and are usually regarded as complex ores since the iron cannot be completely liberated from the iron-oxide matrix even through fine grinding [23–25]. Reduction roasting followed by magnetic separation has been successfully applied to beneficiate these kinds of ores [26–28]. Though magnetite is known to be an excellent MW absorber [29], the MW response of low-grade titano-magnetite ore has not been studied to date.

The present work primarily focuses on comparing the MW-based heating and reduction behaviours of a titano-magnetite ore with those of a goethite rich low-grade ore using high-ash coal as the reductant. The experiments were conducted using a Taguchi-based statistical design. To establish the difference in the MW responses as well as reduction mechanisms, characterization studies were carried out, such as vibrating-sample magnetometry (VSM), X-ray diffraction (XRD), electron-probe microanalysis (EPMA), and optical microscopy (OM).

## 2. Experimental

### 2.1. Samples

The titano-magnetite ore (O1) was collected from Nigeria, while the iron ore overburden sample (O2) was received from Jharkhand, India. The samples were crushed to below 10 mm and riffled to produce representative samples. The chemical analysis results of the respective ore samples are listed in Table 1. A high-ash coal sample (fixed carbon: 34.57 wt%, volatile: 29.11wt%, ash: 23.12wt%, moisture: 13.2wt%) used as the reductant in this study was collected from Talcher, India. The size of the coal was reduced to below 1 mm for all the reduction experiments. The size analysis results of the iron ore and coal sample are presented in Table 2. In the case of O1, the iron content was observed to decrease with the particle size, while for O2, the iron values

**Table 1. Chemical analysis of the two different types of iron ores** wt%

| Iron ore | Fe | $Al_2O_3$ | $SiO_2$ | $TiO_2$ | MgO | LOI |
|---|---|---|---|---|---|---|
| O1 | 49.6 | 6.1 | 7.2 | 13.1 | 1.1 | 1.5 |
| O2 | 49.1 | 10.2 | 7.3 | — | — | 12.3 |

**Table 2. Size analysis results of the iron ore and coal samples**

| Iron Ore | | | | | Coal | | |
|---|---|---|---|---|---|---|---|
| Size / μm | O1 | | O2 | | Size / μm | Weight ratio / wt% | Ash content / wt% |
| | Weight ratio / wt% | Total Fe / wt% | Weight ratio / wt% | Total Fe / wt% | | | |
| −10000+5600 | 15.38 | 51.97 | 33.12 | 49.78 | −1000+500 | 54.83 | 21.45 |
| −5600+3350 | 14.85 | 51.99 | 23.20 | 49.26 | | | |
| −3350+2000 | 11.30 | 50.13 | 13.12 | 49.09 | −500+300 | 14.88 | 23.94 |
| −2000+1000 | 18.41 | 50.89 | 12.96 | 48.65 | | | |
| −1000+500 | 15.59 | 53.53 | 5.60 | 48.51 | −300+150 | 14.10 | 24.58 |
| −500+300 | 8.58 | 50.66 | 3.68 | 48.33 | | | |
| −300+150 | 8.16 | 42.62 | 3.52 | 47.95 | −150+100 | 4.44 | 25.10 |
| −150+100 | 2.30 | 38.92 | 1.12 | 46.99 | | | |
| −100 | 5.44 | 32.96 | 3.68 | 46.98 | −100 | 11.75 | 27.34 |
| Bulk | 100 | 49.60 | 100 | 49.10 | Bulk | 100 | 23.12 |

were found to be almost equally distributed across all the size fractions. In the case of the coal sample, the ash showed a marginal increase in content at finer size fractions.

### 2.2. Microwave-based reduction roasting

The reduction roasting experiments were performed in a laboratory-scale MW system supplied by VB Ceramics Consultants, Chennai. The significant features of the MW furnace are a control panel, a power supply system, an air-cooled magnetron, a circulator with a water load, an aluminium waveguide, and a multimode cavity for sample processing. The MW furnace with a frequency of 2.45 GHz was designed for a maximum power input of 10 kW and a minimum of 1 kW, allowing up to a maximum temperature of 1500ºC. The insulation zone inside the furnace was about 125 mm from all the sides of the chamber and was constructed with vacuum-formed ceramic fibreboard (80wt% $Al_2O_3$ and 20wt% $SiO_2$) supplied by Zircar, USA. This type of insulation enables the furnace to provide a fast heating rate and long soaking hours. The temperature for all the experiments was directly measured using a RAYTEK non-contact Infrared sensor (pyrometer) fixed at the top of the furnace. The pyrometer can sense temperatures ranging from 350 to 1500°C, with the output being connected to a Eurotherm PID controller.

The MW-based reduction experiments were conducted by taking the thoroughly mixed iron ore and coal sample at a scale of 500 g in a tall form quartz crucible. The mixture was kept for a designated time in the MW furnace, operated at a particular power in the presence of air. On completion of each experiment, the roasted ore was quickly removed from the chamber and instantly water-quenched to inhibit re-oxidation. Consequently, the obtained roasted mass was subjected to various characterization techniques such as EPMA, XRD, VSM, and OM.

### 2.3. Magnetic separation

The cooled roasted mass was wet-ground in a laboratory-scale ball mill at a pulp density of 30% to a particle size below 75 µm. The slurry was then subjected to magnetic separation in a wet low-intensity magnetic separation (LIMS) unit supplied by In-Smart Systems, Hyderabad, India, at a magnetic field strength of about 0.15 T. The magnetic and non-magnetic fractions were collected separately, dried and subjected to chemical analysis to determine the Fe grade and yield. The process flow diagram of the entire conducted experimental work is displayed in Fig. 1.

### 2.4. Experimental design

The reduction experiments were designed based on the Taguchi's $L_{16}$ orthogonal arrays using the software MINITAB 14.0. The purpose was to find the levels of the factors responsible for maximizing the Fe grade and Fe recovery of the magnetic product. The signal to noise (S/N) ratios were determined for assessing the process response, i.e., Fe grade and recovery. The details of the factors and their respective levels in the $L_{16}$ design are presented in Table 3.

### 2.5. Characterization techniques

The chemical analyses of the samples were carried out both through wet chemical techniques and X-ray fluorescence (Make-PANalytical, Model-Zetium). The XRD studies of the representative iron ore samples and some of the products were carried out using a Philips diffractometer (PW-1710) with an automatic divergence slit, receiving slit and graphite monochromator assembly. Moreover, Cu $K_\alpha$ radi-

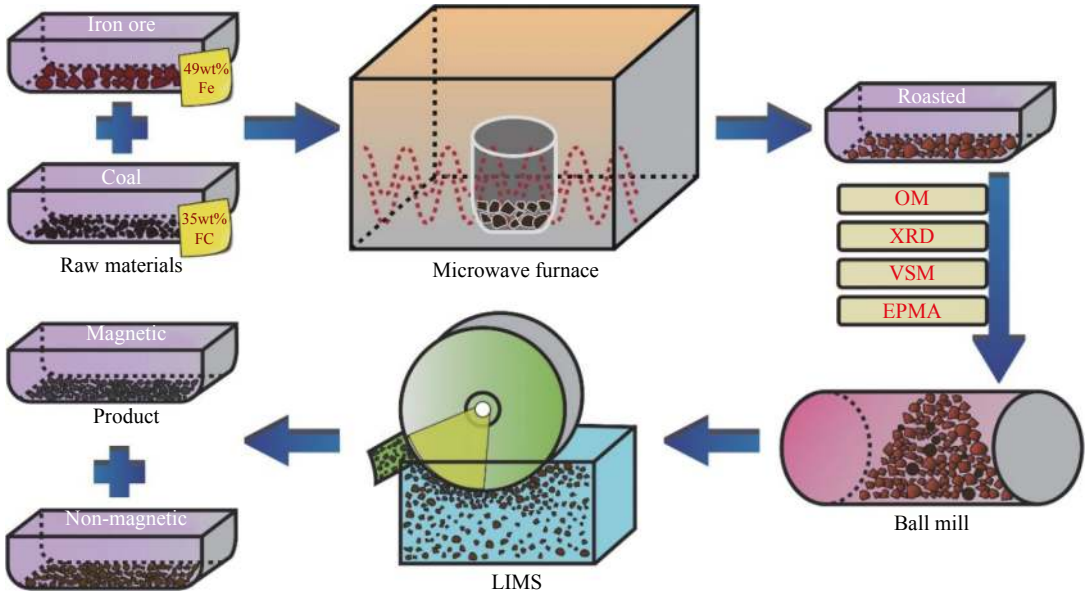


**Fig. 1. Process flow diagram of the experimental work (FC: fixed carbon).**

**Table 3. Assignment of levels of various factors used in the reduction**

| No. | Power / kW | Time / min | Coal-to-ore ratio |
|---|---|---|---|
| Level 1 | 4 | 10 | 0.05 |
| Level 2 | 5 | 15 | 0.10 |
| Level 3 | 6 | 20 | 0.15 |
| Level 4 | 7 | 25 | 0.20 |

ation operating at 40 kV and 20 nA was employed for this work. Reflected-light OM studies were conducted using a Leitz microscope. The EPMA of the ore and some roasted samples were performed using a JEOL superprobe (JXA-8200). The working voltage was maintained at 20 kV with the beam current at 40–100 nA. The elemental distribution in the samples was determined using the X-ray scanning mode. The magnetic properties of the sample before and after roasting were tested using the Princeton VSM (Make-Quantum design) at room temperature. Pulverized mass was placed between the electromagnets, and then the magnetic field was increased to obtain the saturation magnetization (SM) value of the test sample.

## 3. Results and discussion

### 3.1. Characterization of feed

The samples O1 and O2 were subjected to XRD and OM analyses to determine the constituent phases. As evident from the XRD pattern shown in Fig. 2(a), the O1 sample contained magnetite and ilmenite as the major minerals. The corresponding optical micrograph (Fig. 2(b)) shows that the magnetite phase was not homogeneous and contained minute intergrowths of ilmenite. Magnetite was the dominant primary oxide mineral phase occurring as irregular massive grains. It was identified by its greyish white colour with a pinkish tinge and its non-pleochroic as well as isotropic nature, as observed under plane-polarized light. The magnetite was also observed to contain an exsolution texture in the form of lamellar ilmenite. It was characterised by the development of lamellar and the emulsion intergrowth of ilmenite. Isolated grains of magnetite without intergrowth were rarely seen in this sample. The feed sample featured fine lamellar intergrowth of ilmenite, with magnetite forming "Widmanstatten texture" or "Trellis intergrowth" (Fig. 2(b)). The lamellar intergrowth generally forms because of the unmixing or exsolution between these two phases [30].

On the other hand, as revealed from the XRD pattern given in Fig. 2(c), the O2 sample is a goethite-dominated ore associated with hematite, kaolinite, and quartz. Goethite is usually formed under oxidizing conditions as a weathering product of iron-bearing minerals, through inorganic or organic precipitation. In this sample, alternate colloform layers of goethite were found to be well developed (Fig. 2(d)), with the

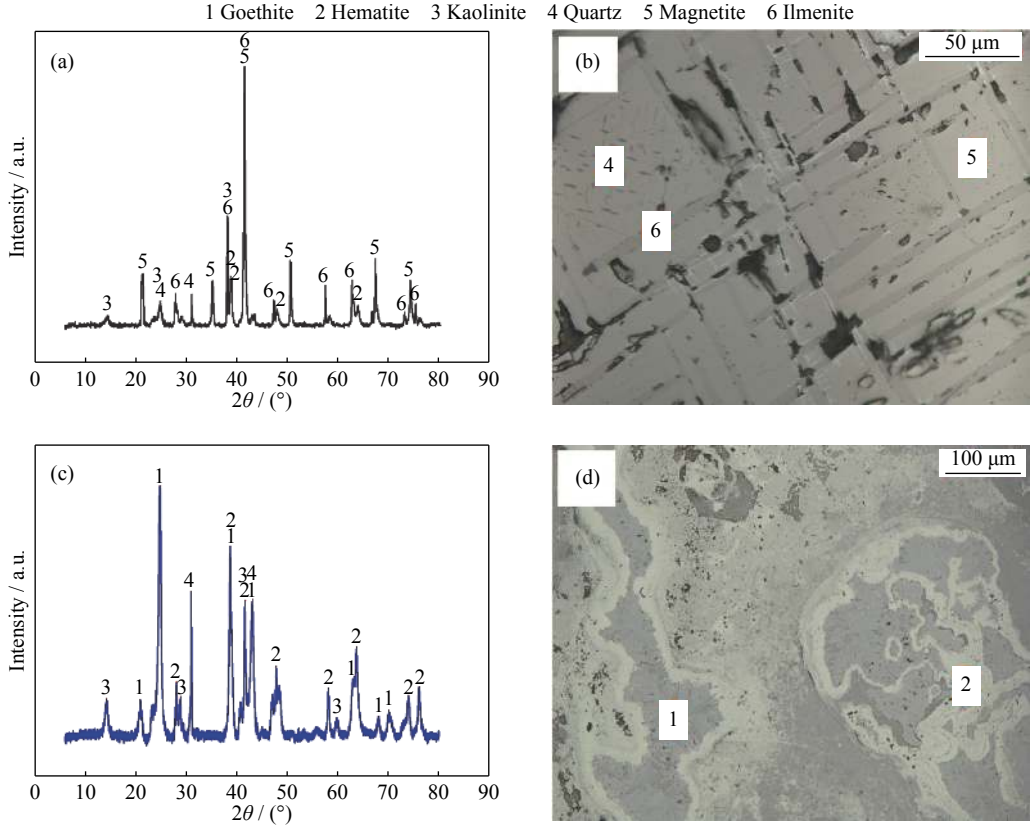


**Fig. 2. XRD patterns and optical micrographs of the feed ores: (a, b) O1; (c, d) O2.**

layers having varying thicknesses and reflectivities. Rhythmic concentric layers of goethite in different shades were also present. Both massive and colloidal forms of goethite were observed in this sample. The presence of hematite in the periphery of the goethite suggests the possible dehydration of the latter, leading to the formation of hematite.

### 3.2. Microwave-based reduction roasting of O1 and O2 ores

The reduction roasting–magnetic separation experiments were conducted as per the $L_{16}$ design, and the corresponding results in terms of the Fe grade and recovery of the magnetic products are given in Table 4. Comparing the grade and recovery for both ores, O1 responded reasonably better than O2 in the MW-assisted reduction roasting followed by magnetic separation. The results indicate that ore O1 could be upgraded to 62.88wt% Fe with 62.19% Fe recovery. Though the experiments were yielding higher Fe recovery, the conditions were not adequate to yield Fe content in the range of 63wt%–64wt%. However, in the case of O2, the grades obtained were not very impressive since the best concentrate was obtained with only 60.2wt% Fe and 66.32% Fe recovery. Moreover, ore O2 needed more MW power and residence time to achieve a Fe grade of 60.20%. The results were further subjected to statistical analyses to clarify the roles of different factors in the reducing behaviour of both ores.

**Table 4. Iron grade and recovery response from statistically designed experiments**

| Exp. No. | Experimental conditions | | | O1 + Coal | | O2 + Coal | |
|---|---|---|---|---|---|---|---|
| | Power / kW | Time / min | Coal-to-ore ratio | Grade / % | Recovery / % | Grade / % | Recovery / % |
| 1 | 4 | 10 | 0.05 | 61.59 | 72.59 | 59.57 | 6.48 |
| 2 | 4 | 15 | 0.10 | 60.14 | 77.40 | 59.51 | 11.33 |
| 3 | 4 | 20 | 0.15 | 61.31 | 58.97 | 58.97 | 36.89 |
| 4 | 4 | 25 | 0.20 | 60.47 | 66.36 | 57.24 | 24.13 |
| 5 | 5 | 10 | 0.10 | 58.97 | 74.30 | 58.73 | 21.57 |
| 6 | 5 | 15 | 0.05 | 61.08 | 55.44 | 59.89 | 20.36 |
| 7 | 5 | 20 | 0.20 | 62.88 | 62.19 | 58.36 | 80.16 |
| 8 | 5 | 25 | 0.15 | 66.85 | 51.62 | 59.17 | 61.96 |
| 9 | 6 | 10 | 0.15 | 62.24 | 66.61 | 58.06 | 52.11 |
| 10 | 6 | 15 | 0.20 | 65.34 | 54.00 | 59.14 | 48.50 |
| 11 | 6 | 20 | 0.05 | 64.11 | 40.82 | 58.41 | 78.64 |
| 12 | 6 | 25 | 0.10 | 63.22 | 59.10 | 58.35 | 66.66 |
| 13 | 7 | 10 | 0.20 | 59.67 | 65.48 | 58.32 | 46.00 |
| 14 | 7 | 15 | 0.15 | 70.55 | 43.01 | 57.78 | 62.86 |
| 15 | 7 | 20 | 0.10 | 66.59 | 29.77 | 59.32 | 76.47 |
| 16 | 7 | 25 | 0.05 | 65.25 | 45.08 | 60.20 | 66.32 |

Fig. 3 shows the impact of the factors on the grade and recovery of both ore types, i.e., O1 and O2. The main effects, as well as the delta plot, indicate that the MW power and exposure time are the most significant parameters, while the coal-to-ore ratio has a relatively less substantial influence. The delta value, which is the difference between the highest and the lowest S/N ratio, denotes the relative significance of a factor. It is evident from the main effects plot that the mean S/N ratio for O1, which was calculated considering both Fe grade and recovery as the responses, decreased as the MW power increased from 4 to 7 kW. In contrast, in the case of O2, the mean S/N ratio rose with the same increase in MW power. This variation in effect may be attributed to the difference in the mineralogical characteristics of O1 and O2. Although a similar trend can also be seen in the case of the exposure time of MW radiation, for O1, the mean S/N ratio increased with an increase in time from 20 to 25 min. This trend is because of the rise in iron grade and the marginal effect on the recovery at an exposure time of 25 min (Table 3). The mean S/N ratios obtained at different coal-to-ore ratios for O1 did not vary significantly, and hence, the ratio had less impact on the iron grade and recovery as compared to MW power and time. However, the rise in mean S/N ratios at a high coal-to-ore ratios, i.e., 0.15 and 0.20, for O2, suggests that ore O2 is not as amenable to MW radiation as O1. Thus, the MW heating profiles of both ore types were studied further to comprehend the above-discussed results.

### 3.3. Microwave heating studies of ores with response to coal addition

The temperatures of the O1 and O2 ores versus MW heating time are shown in Fig. 4. Though both ores were heated well in response to the MW treatment, O1 was heated significantly better than O2. For example, at an MW power of 5 kW, ore O1 could reach a maximum temperature of about 727°C after 30 min heating time, while ore O2 exhibited an utterly different behaviour, with the maximum temperature around 600°C. Similarly, ore O1 showed better heating characteristics than O2 at a higher MW power of 7 kW. Moreover, ore O1 had a higher initial heating rate, which de-

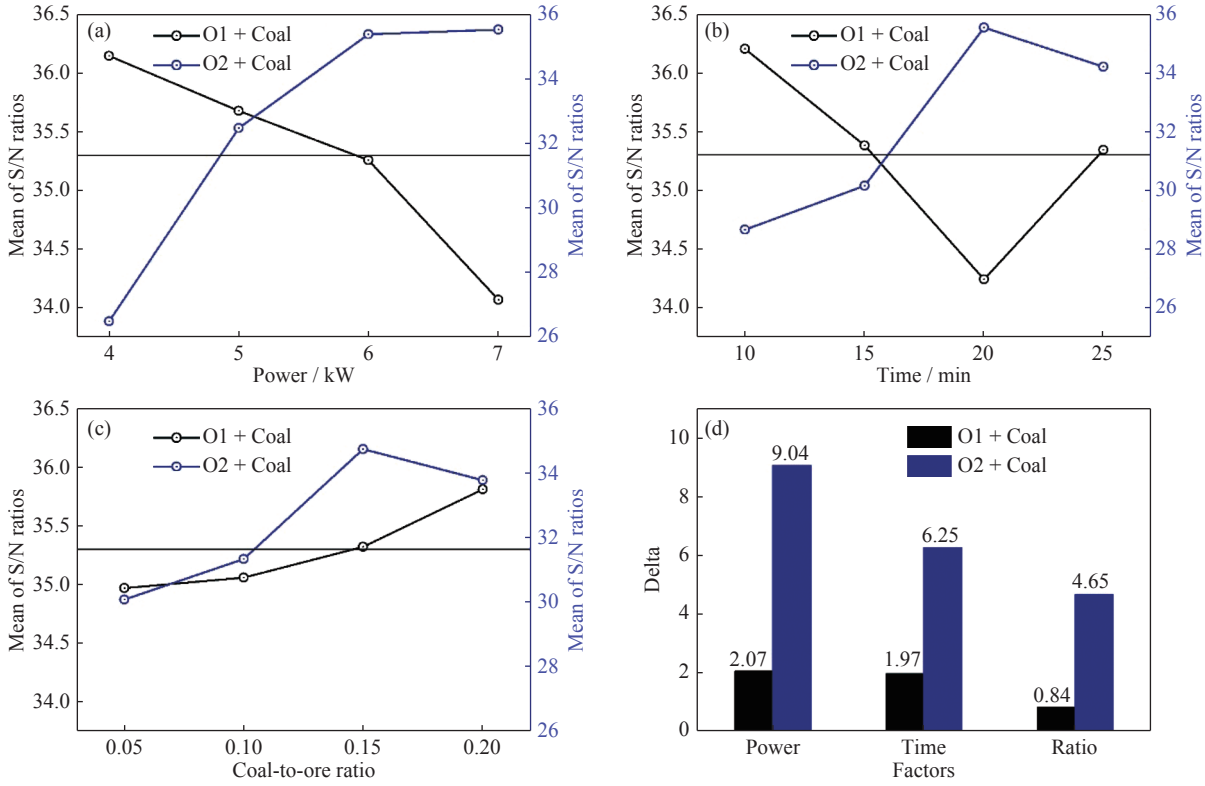


**Fig. 3. Main effects plot showing the variation in S/N ratio as a function of different factors: (a) MW power, (b) time, (c) coal-to-ore ratio, and (d) delta values as calculated for the $L_{16}$ MW reduction roasting experiments for O1 + Coal and O2 + Coal.**

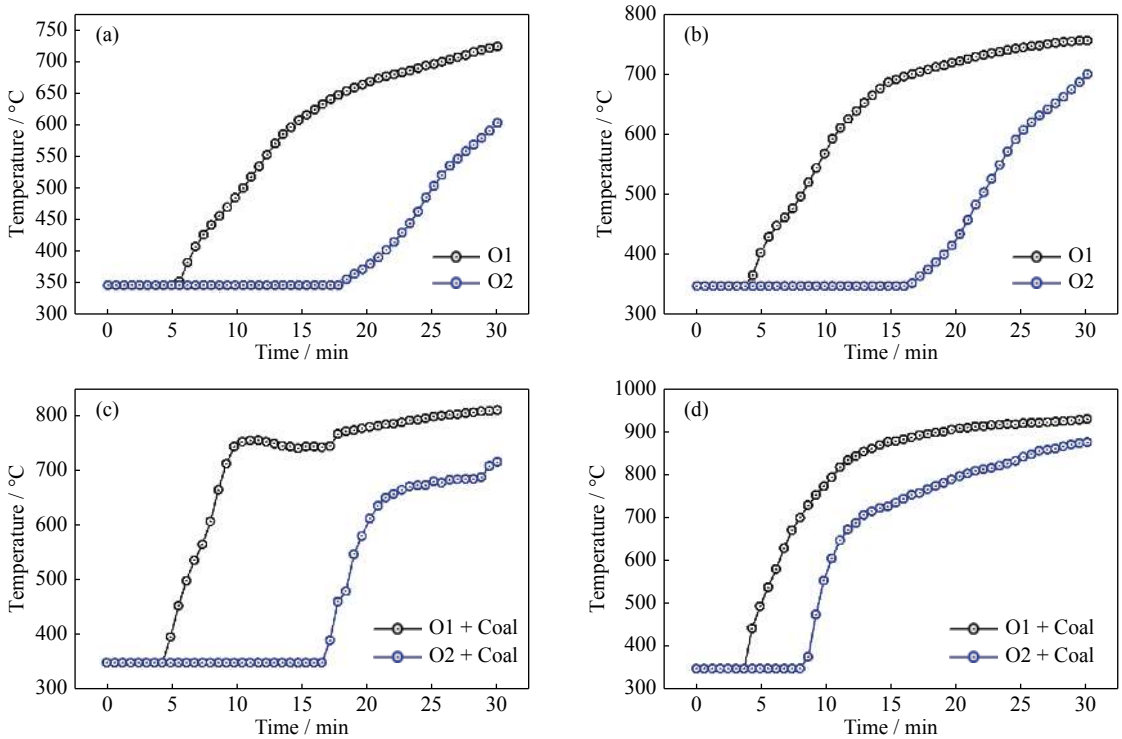


**Fig. 4. Microwave heating behaviour of raw ores O1 and O2 roasted at an MW power of (a) 5 kW and (b) 7 kW and roasted with addition of coal (0.2 coal-to-ore ratio) at an MW power of (c) 5 kW and (d) 7 kW.**

clined gradually with the increase in MW exposure time; this heating characteristic of O1 is the main reason for the better reduction even at low MW power as well as time. From Fig. 4, it can also be inferred that the temperature of O1 when

it was roasted along with coal almost reached 800°C at an MW power of 5 kW and time of 20 min. In contrast, the poor heating characteristic of O2 led to a maximum temperature of about 700°C when it was roasted with coal. Therefore, the iron oxides present in O2, such as goethite, could not be sufficiently converted to magnetite, and poor iron grade and recovery was obtained. However, at a high MW power of 7 kW, ore O2 showed better results since the temperature reached around 850°C after 25 min of MW exposure. Meanwhile, the temperature for O1 crossed around 900°C after 15 min of roasting with coal and thus facilitated the formation of phases such as wustite and iron metal. A detailed study of the reduction sequence and formation of different phases using several characterization techniques was therefore undertaken and was discussed in the following section.

### 3.4. Characterization of the roasted samples

Characterization studies were conducted for samples O1 and O2 roasted at two sets of conditions, given in Table 5. Also given in the table are the corresponding Fe grades and Fe recoveries obtained as a result of the LIMS of the respective roasted mass. For OM, EPMA, and VSM analyses, the roasted mass was used as the test sample, while magnetic and non-magnetic samples separated through LIMS were subjected to XRD analysis.

The relative XRD patterns of the magnetic and non-magnetic fractions are shown in Fig. 5. The magnetic fraction of O1 MW-roasted under 5 kW power and 15 min and with a coal-to-ore ratio of 0.2 shows magnetite as the significant phase along with a small amount of wustite and metallic iron (Fig. 5(a)). The corresponding non-magnetic fraction primarily contained ilmenite and quartz, with traces of wustite (Fig. 5(b)). This suggests that the hematite present in feed O1 was converted to magnetite, whereas a part of the magnetite already existing in the feed was reduced to wustite and metallic iron. Even though wustite is feebly magnetic, it possibly occurred in the magnetic fraction owing to its close association with magnetite. The presence of metallic iron and wustite in the product indicates the corresponding reducing conditions to be more than sufficient for the magnetization of

**Table 5. Experimental conditions to generate roasted samples for characterization studies with the corresponding results of LIMS in terms of Fe grade and recovery (the coal-to-ore ratio is fixed at 0.2)**

| Sample | Experimental conditions | | Grade / % | Recovery / % |
|---|---|---|---|---|
| | Power / kW | Time / min | | |
| O1 + Coal | 5 | 15 | 62.57 | 60.01 |
| | 7 | 25 | 67.90 | 44.34 |
| O2 + Coal | 5 | 15 | 59.02 | 16.86 |
| | 7 | 25 | 64.40 | 33.30 |

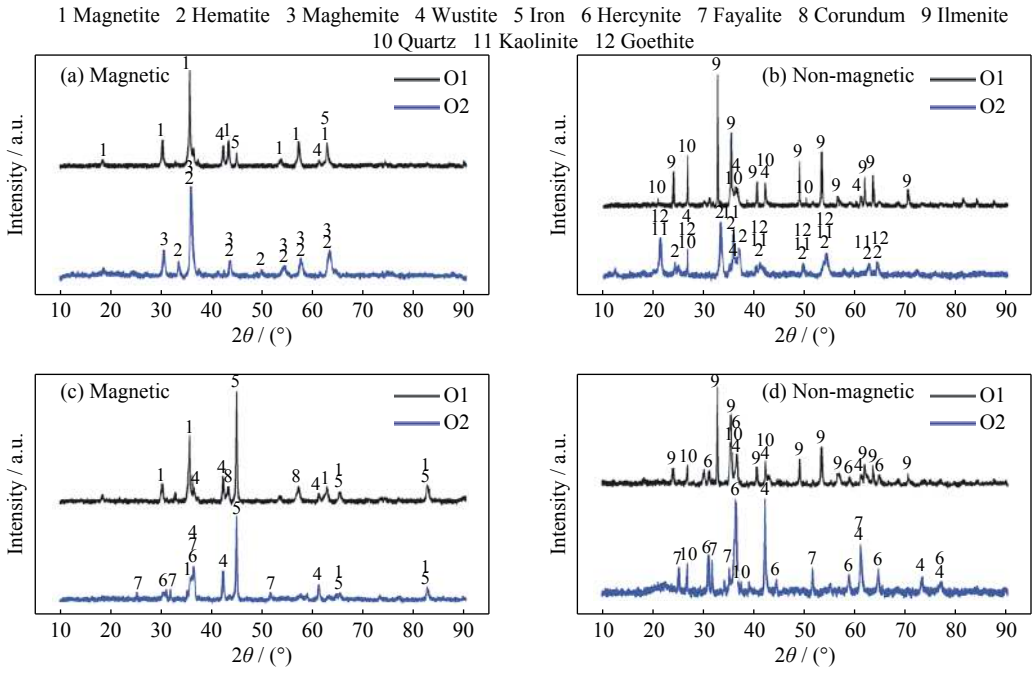


**Fig. 5. XRD patterns of magnetic and non-magnetic concentrates obtained from the reduction roasting of O1 and O2 under the following conditions: (a, b) power of 5 kW and time of 15 min; (c, d) power of 7 kW and time of 25 min.**

the hematite phases present in feed O1. The Fe grade and Fe recovery values of 62.57% and 60.01%, respectively, obtained from O1 at these conditions validate the findings from XRD.

On the other hand, the magnetic fraction obtained from sample O2 roasted at the same conditions shows the presence of hematite and maghemite (Fig. 5(a)). Maghemite is an intermediate phase formed between hematite to magnetite conversion, and its presence in the product infers that the roasting conditions were not adequate for producing magnetite. This is evident from a Fe grade of 59.02% and a poor Fe recovery of 16.86% for the magnetic product obtained from the MW roasting–magnetic separation of O2 at these conditions. Moreover, the presence of hematite, goethite, and kaolinite in the corresponding non-magnetic fraction (Fig. 5(b)) suggests the conditions were not appropriate even for the complete dehydration of the phases. In the XRD pattern of the magnetic fraction of O1 roasted under 7 kW power, 25 min, and with a coal-to-ore ratio of 0.2 (Fig. 5(c)), metallic iron appeared to be the major phase along with magnetite. This agrees with the relevant magnetic product, with a high Fe grade of 67.90% and 44.34% Fe recovery obtained at these conditions. The magnetic fraction also contained a minor amount of corundum ($Al_2O_3$), which forms when kaolinite fragments at high temperatures. The XRD pattern of the concerned non-magnetic fraction, as shown in Fig. 5(d), shows peaks similar to those of Fig. 5(b), with hercynite ($FeAl_2O_4$) being an addition. Hercynite is a phase formed as a result of the reaction between iron oxide and kaolinite at the higher reducing conditions. The XRD pattern of the magnetic product of O2 roasted at the same conditions mostly includes metallic iron and magnetite, along with wustite and fayalite ($Fe_2SiO_4$). This magnetic product had a grade of 64.40% Fe with 33.30% Fe recovery, which were higher than those of the product obtained from the previous conditions (5 kW power, 15 min, and coal-to-ore ratio 0.2). Though fayalite is paramagnetic, its presence in the magnetic part is possibly due to its intimate association in the ferromagnetic rich area. Quartz, wustite, hercynite, and fayalite are found to be present in the non-magnetic portion of ore O2 (Fig. 5(d)). The XRD studies show the formation of several magnetic and non-magnetic minerals at two different sets of MW roasting conditions and validate the corresponding obtained Fe grade and recovery of the products.

To further validate the formation of the phases and understand their association with each other, reflected-light microscopy studies of the roasted products obtained at the same conditions were undertaken, and the corresponding micrographs are displayed in Fig. 6.

In sample O1, most of the grains were partially or wholly martitized, mainly along the grain boundaries and the weak planes of ilmenite. The magnetite showed a pitted appearance, having a lot of silicate inclusions (Fig. 6(a)). Perfect euhedral to subhedral crystals of ilmenite exhibiting mutual

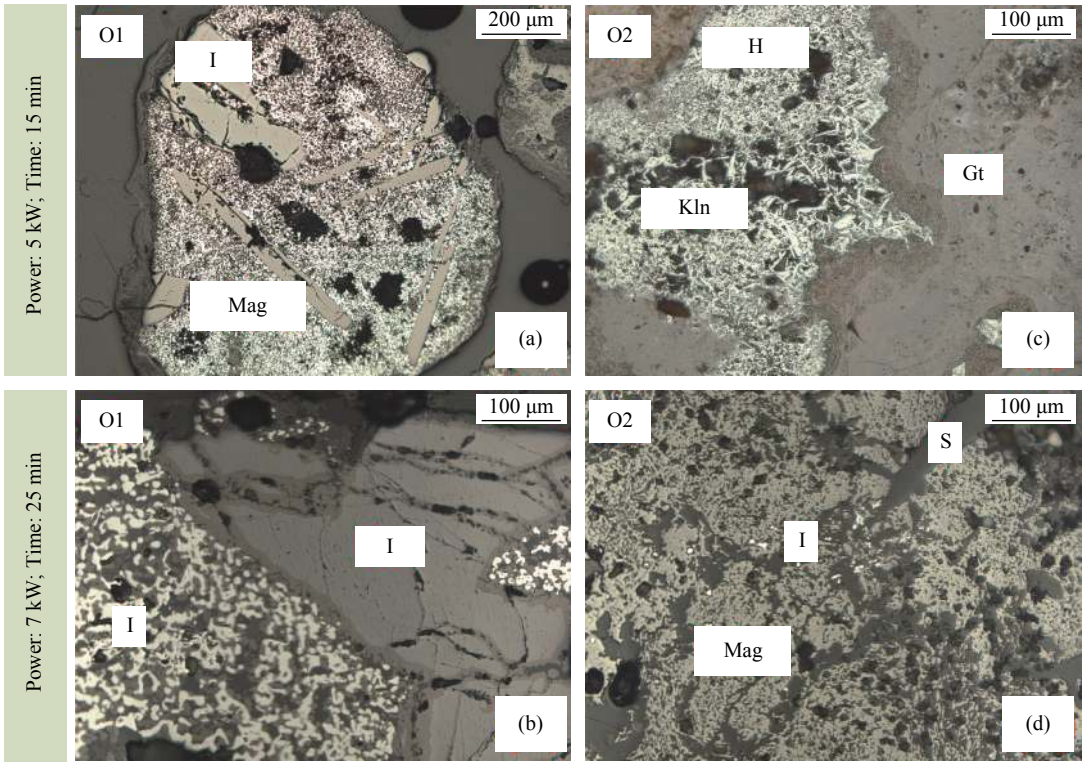


**Fig. 6. Mineral phases identified by optical microscopy for the reduced iron ore sample of both (a, b) O1 and (c, d) O2 at two different reducing conditions (Gt: goethite, Kln: kaolinite, H: hematite, I: ilmenite, S: silicates, and Mag: magnetite).**

boundary texture with magnetite was noticed. With the increase in power and time, the concentration of iron-rich phase was increased to form wustite or metallic iron (Fig. 6(b)) along with the formation of iron silicates both in the contact boundaries and the fracture planes of ilmenite and the metallic phase as well as within the open spaces between metallic phases.

In sample O2, under 5 kW power and 15 min, mostly massive goethite phases were seen together with the needle-shaped fine-grained hematite with some clay patches in between (Fig. 6(c)). With the increase in power and time, the hematite and goethite were all converted to magnetite, and some silicates (Fe/Al-silicates) were present as fillings (Fig. 6(d)). The presence of the metallic phase is almost negligible when compared with the case of O1 roasted under the same conditions.

The elemental distribution maps of feed ores O1 and O2 accompanied by their roasted products are illustrated in Figs. 7 and 8, respectively. For sample O1, the backscattered electron image with Fe, Ti, and Al mapping explains the presence of some Al as impurities dispersed within the iron phase. Titanium- and Fe-bearing phases showed uniform distribution, which typically represent the ilmenite phase (Fig. 7(a)). However, the electron mapping of the roasted product shown in Fig. 7(b) explains the dispersion of iron particles in the groundmass containing laths of ilmenite. Some Al minerals were also adsorbed within the iron phases. With the increase in time and power, the formation of metal-

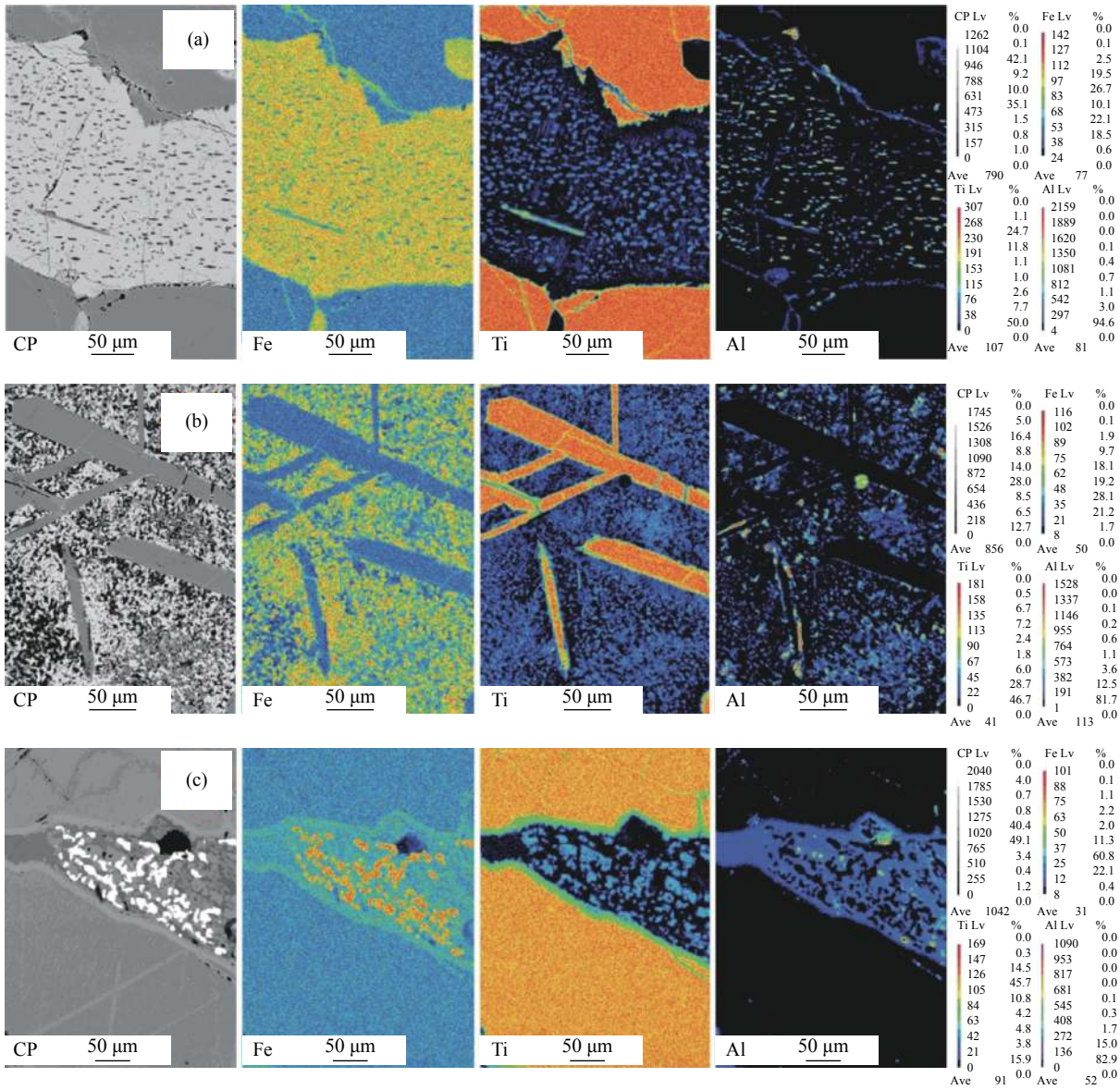


**Fig. 7. EPMA-based elemental mapping of ore sample O1: (a) feed ore; product roasted at MW conditions of (b) 5 kW and 15 min and (c) 7 kW and 25 min with coal-to-ore ratio of 0.2.**

lic iron is clear from the Fe map of Fig. 7(c).

The elemental mapping of the O2 sample describes the concentrations of Fe, Al, and Si present in the feed as well as in the roasted products. Fig. 8(a) shows a typical colloidal band of goethite, which mostly comprises Fe. The presence of an Al phase within the goethite band indicates the close association of kaolinite with goethite. At conditions such as 5 kW power and 15 min time, dehydration started with the formation of iron oxides and Al silicate as marked in the sample (Fig. 8(b)). The formation of iron-rich phases such as magnetite and metallic iron/wustite was marked in the sample roasted at 7 kW power and 25 min period (Fig. 8(c)). The red dots in the Fe map of Fig. 8(c) confirms the little presence of the metallic iron phase in this condition. Comparing the elemental mappings of the O1 and O2 roasted products, it is evident that O2 had less metallic Fe and more Al silicate phases embedded in the magnetite matrix, explaining why the magnetic separation in the case of O2 could not yield a high iron recovery like O1.

### 3.5. Magnetic properties of roasted samples

The SM is considered to be an essential parameter that determines to which extent a substance can respond to magnetic separation. Therefore, samples O1 and O2 were subjected to VSM to understand the effect of MW heating with and without the reductant. Fig. 9 shows the SM values of the ores treated at different MW exposure periods, from 10 to 25 min, at a fixed power of 5 kW. As sample O1 had a majority of its

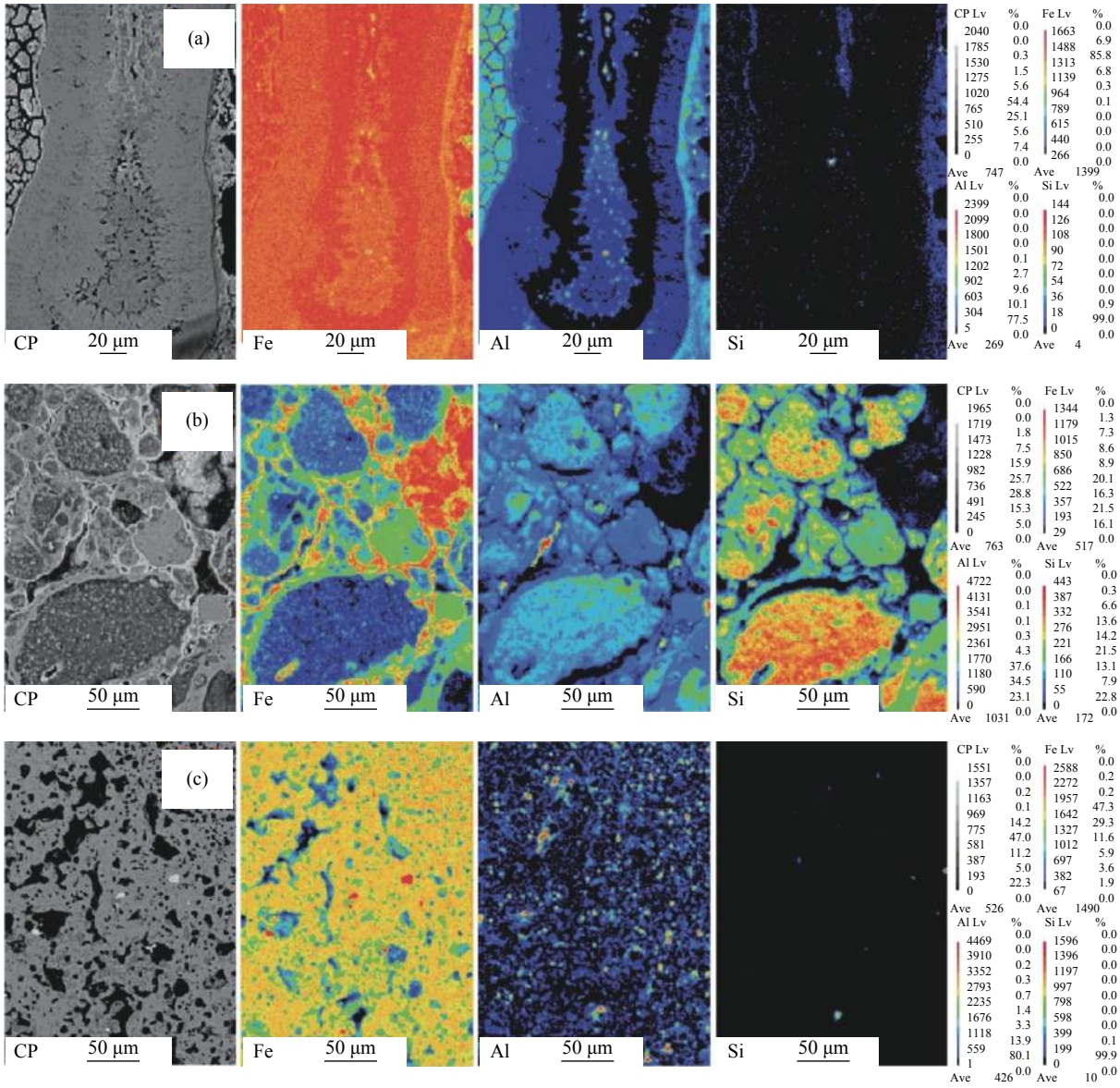


**Fig. 8. EPMA-based elemental mapping of ore sample O2: (a) feed ore; product roasted at MW conditions of (b) 5 kW and 15 min and (c) 7 kW and 25 min with coal-to-ore ratio of 0.2.**

iron oxides in the form of magnetite, the SM value was found to be 0.0055 A/m. When O1 was treated in MW without any reductant, the SM value gradually decreased to 0.0043 A/m (Fig. 9(a)). This is mainly attributed to the partial oxidation of the magnetite present in the ore to hematite ($2Fe_3O_4 + O_2 \rightarrow 3Fe_2O_3$), which has less magnetic susceptibility compared with the former. In contrast, when O2 was MW-treated at four different time intervals, the SM increased to a maximum of 0.001 A/m. This increase is basically due to the thermal decomposition of goethite into hematite ($2FeOOH \rightarrow Fe_2O_3 + H_2O$), which is considered more magnetic than goethite.

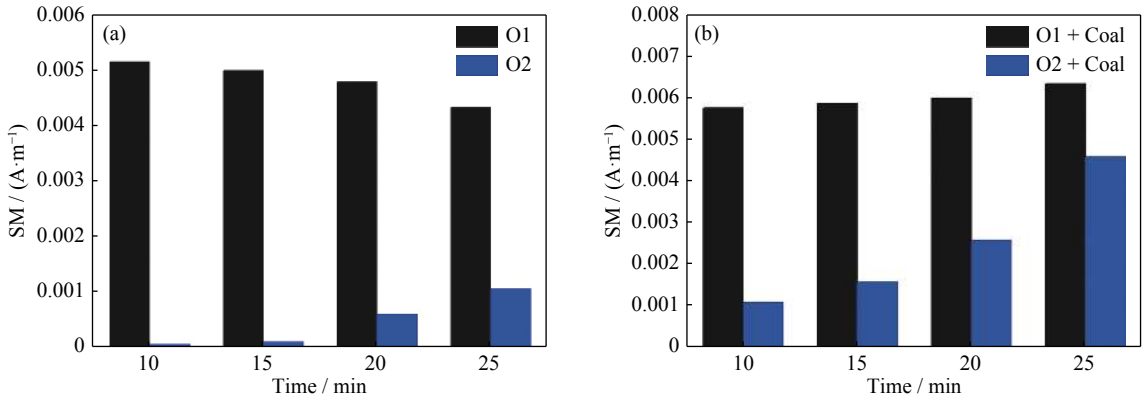


**Fig. 9. Effect of MW exposure on saturation magnetisation of (a) feed ore O1 and O2 and (b) feed ore O1 and O2 with coal-to-ore ratio of 0.2 at a power of 5 kW.**

The SM values of the products roasted using coal as a function of time are depicted in Fig. 9(b). Coal addition enhanced the SM of both the roasted samples. The improved values were mostly due to the phase transformation of the feeble magnetic minerals into higher magnetic susceptible products, as already confirmed through the XRD and microscopy studies. In the case of O1, the SM slightly increased, resulting in a maximum of about 0.0063 A/m for a period of 25 min. On the contrary, the goethite-rich O2 ore could experience a maximum SM of 0.0046 A/m even at a period of 25 min. These results further confirm that the O2 ore needs higher MW exposure time to realize sufficient magnetization to enable separation into a useful magnetic concentrate.

### 3.6. Microwave-based reduction roasting of ore mixtures

The results discussed so far suggest that using MW-assisted reduction roasting followed by magnetic separation, it is easier to obtain a suitable iron ore concentrate from O1 than from O2. This is primarily because of the presence of magnetite and ilmenite in the former, which are MW-absorbing minerals [31]. In the case of O2, where goethite (α-FeOOH) is mostly present, the MW heating leads to its decomposition to hematite (α-$Fe_2O_3$) and water. Therefore, during the initial stage of thermal transformation, the real and imaginary permittivity values are very low, but with increasing temperature, the rate of water removal increases as the flux of migrating hydroxyl unit increases, improving the MW absorbing characteristics of the ore [32–34]. This explains why the MW-assisted heating or reduction in the case of the goethite-rich O2 is less than that in the case of O1.

Further attempts were made to blend these samples and subject to MW roasting followed by magnetic separation. Fig. 10(a) shows the response of the ore mixtures in terms of Fe grade and recovery, which were obtained by subjecting the mixtures to 5 kW power for a period of 25 min, with a coal-to-ore ratio of 0.2. With increasing amount of O2 in the mixture, the iron grade decreased and the recovery increased (Fig. 10(a)). Considering both the iron grade and recovery, the mixture of 60:40 (O2 : O1), corresponding to a grade of 65.19% Fe at a total Fe recovery of 56.75%, was chosen as the optimum level. Furthermore, this ore mixture was subjected to different MW exposure times at 5 kW power. The impact of time on the iron grade and recovery is shown in Fig. 10(b). At an exposure time of 15 min, a magnetite concentrate of 61.57wt% Fe with 64.47% iron recovery could be obtained. However, on increasing the time beyond 15 min, the recovery dropped even though the Fe grade rose. Therefore, an exposure time of 15 min at 5 kW MW power and a ratio of 60:40 (O2 : O1) were found to be ideal. Overall, by blending with O1, the O2 ore, which could be enriched to a maximum of 64.40wt% Fe with only 33.30% iron recovery at a power of 7 kW, could present a higher recovery of 64.47% with a slight drop in grade to 61.57% Fe.

To summarise, the grade versus recovery plot for ores O1 and O2 and ore mixture at different MW process parameters is shown in Fig. 11. The plot depicts the grade recovery results listed in Table 5 and that obtained with the optimum ratio of O1 and O2. Ore O1 gave a high Fe grade along with a low Fe recovery at an MW power of 7 kW and a period of 25 min. At the same conditions, O2 showed a lower grade as well as recovery. At an MW power of 5 kW and a period of 15 min, ore O1, in comparison to O2, displayed a better re-

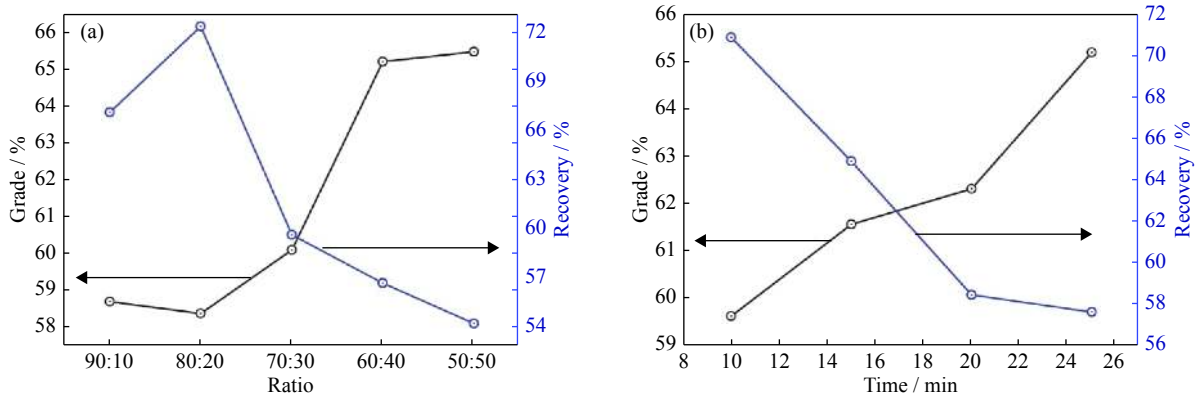


**Fig. 10. Variation of grade and recovery in (a) different ratios of O2 and O1 (O2 : O1) and (b) different levels of time with a constant mixture of 60:40 (O2 : O1).**

sponse in terms of grade and recovery. Nevertheless, the highest recovery of 64.47% with 61.57wt% Fe could only be achieved with the 60:40 (O2 : O1) ore mixture at 5 kW and 15 min. Moreover, at these MW conditions, the energy consumption was 1.2 kW·h. The grade–recovery plot hints that when dealing with goethite-rich ores such O2 in MW-aided reduction roasting processes, they should be blended with magnetite-rich ores (such as O1 in this case) to obtain the perfect combination of iron grade and recovery.

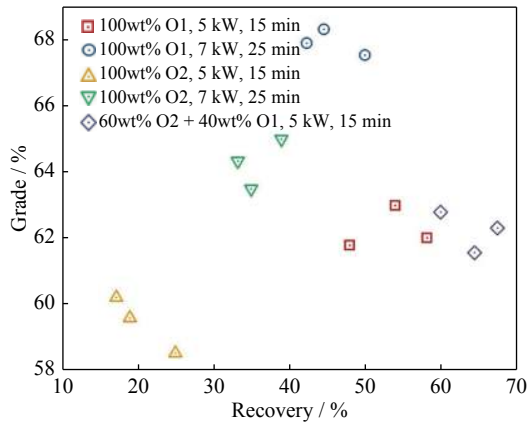


**Fig. 11. Grade–recovery plot for O1 and O2 at different MW reducing conditions.**

## 4. Conclusions

This study attempted to upgrade the iron contents of two low-grade iron ores via MW-assisted reduction roasting followed by magnetic separation process. The research addressed the issues and complications related to the development of an MW process for iron ores with mineralogical variations. The key findings of the work are listed below.

(1) Under a power of 5 kW, coal-to-ore ratio of 0.2, and time of 15 min, the titano-magnetite ore was upgraded to feature an iron content of 62.57wt% with Fe recovery of 60.01%, whereas under the same conditions, the goethite ore yielded a recovery of 16.80%. This indicates that mineralogy plays a crucial role in MW heating.

(2) The VSM studies revealed that magnetizing the goethite-rich sample is difficult as it took around 25 min at 7 kW MW power to reach an SM value of 0.0046 A/m, which was even lesser than the SM value of the untreated titano-magnetite ore.

(3) The blend of the two ores prepared by mixing the goethite rich ore with the titano-magnetite ore in a 60:40 (O2 : O1) ratio could be upgraded to feature 61.57wt% Fe at an MW power of 5 kW and time of 15 min with a coal-to-ore ratio of 0.2. This infers that the blending of a low-grade magnetite rich ore could improve the results of the MW-assisted magnetizing roasting process of low-grade ores that do not suitably absorb MW.

(4) Reduction roasting followed by magnetic separation is one of the most effective ways to upgrade the iron content of poorly liberated ores. In this regard, the present work can be considered as a preliminary endeavour to introduce MW energy in the reduction-roasting of such ores. More efforts are required to establish the process on a larger scale and calculate the energy consumption and viability for commercial exploitation.

## Acknowledgements

The authors are thankful to the Director, CSIR-IMMT, Bhubaneswar for his permission to publish this paper and the Ministry of Steel, Government of India, for their financial support (F. No. 11(12)/GBS/2014-TW).

## References

[1] Y.S. Sun, Y.X. Han, P. Gao, Z.L. Wang, and D.Z. Ren, Recovery of iron from high phosphorus oolitic iron ore using coal-based reduction followed by magnetic separation, *Int. J. Miner. Metall. Mater.*, 20(2013), No. 5, p. 411.

[2] G. Wang, Q.G. Xue, and J.S. Wang, Carbothermic reduction characteristics of ludwigite and boron–iron magnetic separation,

*Int. J. Miner. Metall. Mater.*, 25(2018), No. 9, p. 1000.
[3] S.S. Rath, D.S. Rao, S.K. Tripathy, and S.K. Biswal, Characterization vis-á-vis utilization of blast furnace flue dust in the roast reduction of banded iron ore, *Process Saf. Environ. Prot.*, 117(2018), p. 232.
[4] N. Ray, D. Nayak, N. Dash, and S.S. Rath, Utilization of low-grade banded hematite jasper ores: Recovery of iron values and production of ferrosilicon, *Clean Technol. Environ. Policy*, 20(2018), No. 8, p. 1761.
[5] Y.S. Sun, Y.F. Li, Y.X. Han, and Y.J. Li, Migration behaviors and kinetics of phosphorus during coal-based reduction of high-phosphorus oolitic iron ore, *Int. J. Miner. Metall. Mater.*, 26(2019), No. 8, p. 938.
[6] S.M.J. Koleini and K. Barani, Microwave heating applications in mineral processing, [in] W.B. Cao, ed., *The Development and Application of Microwave Heating*, InTechOpen, London, 2012.
[7] K. Onol and M.N. Saridede, Investigation on microwave heating for direct leaching of chalcopyrite ores and concentrates, *Int. J. Miner. Metall. Mater.*, 20(2013), No. 3, p. 228.
[8] Y.Z. Yuan, Y.M. Zhang, T. Liu, and T.J. Chen, Comparison of the mechanisms of microwave roasting and conventional roasting and of their effects on vanadium extraction from stone coal, *Int. J. Miner. Metall. Mater.*, 22(2015), No. 5, p. 476.
[9] K.E. Haque, Microwave energy for mineral treatment processes—A brief review, *Int. J. Miner. Process.*, 57(1999), No. 1, p. 1.
[10] C.A. Pickles, Microwave heating behaviour of nickeliferous limonitic laterite ores, *Miner. Eng.*, 17(2004), No. 6, p. 775.
[11] Z.Q. Zhu and J. Zhou, Rapid growth of ZnO hexagonal tubes by direct microwave heating, *Int. J. Miner. Metall. Mater.*, 17(2010), No. 1, p. 80.
[12] C.A. Pickles, Microwaves in extractive metallurgy: Part 1—Review of fundamentals, *Miner. Eng.*, 22(2009), No. 13, p. 1102.
[13] F.F. Wu, Z.F. Cao, S. Wang, and H. Zhong, Novel and green metallurgical technique of comprehensive utilization of refractory limonite ores, *J. Cleaner Prod.*, 171(2018), p. 831.
[14] V. Rayapudi, S. Agrawal, and N. Dhawan, Optimization of microwave carbothermal reduction for processing of banded hematite jasper ore, *Miner. Eng.*, 138(2019), p. 204.
[15] S.S. Rath, N. Dhawan, D.S. Rao, B. Das, and B.K. Mishra, Beneficiation studies of a difficult to treat iron ore using conventional and microwave roasting, *Powder Technol.*, 301(2016), p. 1016.
[16] P. Kumar, B.K. Sahoo, S. De, D.D. Kar, S. Chakraborty, and B.C. Meikap, Iron ore grindability improvement by microwave pre-treatment, *J. Ind. Eng. Chem.*, 16(2010), No. 5, p. 805.
[17] J.P. Wang, T. Jiang, Y.J. Liu, and X.X. Xue, Influence of microwave treatment on grinding and dissociation characteristics of vanadium titano-magnetite, *Int. J. Miner. Metall. Mater.*, 26(2019), No. 2, p. 160.
[18] J.A. Menéndez, A. Arenillas, B. Fidalgo, Y. Fernández, L. Zubizarreta, E.G. Calvo, and J.M. Bermúdez, Microwave heating process involving carbon materials, *Fuel Process. Technol.*, 91(2010), No. 1, p. 1.
[19] P.C. Beuria, S.K. Biswal, B.K. Mishra, and G.G. Roy, Study on kinetics of thermal decomposition of low LOI goethetic hematite iron ore, *Int. J. Min. Sci. Technol.*, 27(2017), No. 6, p. 1031.
[20] S.K. Das, B. Das, R. Sakthivel, and B.K. Mishra, Mineralogy, microstructure, and chemical composition of goethites in some iron ore deposits of orissa, India, *Miner. Process. Extr. Metall. Rev.*, 31(2010), No. 2, p. 97.
[21] D. Nayak, N. Dash, N. Ray, and S.S. Rath, Utilization of waste coconut shells in the reduction roasting of overburden from iron ore mines, *Powder Technol.*, 353(2019), p. 450.
[22] J.W. Yu, Y.X. Han, Y.J. Li, and P. Gao, Recent advances in magnetization roasting of refractory iron ores: A technological review in the past decade, *Miner. Process. Extr. Metall. Rev.*, 41(2020), No. 5, p. 349.
[23] B.C. Jena, W. Dresler, and I.G. Reilly, Extraction of titanium, vanadium and iron from titanomagnetite deposits at pipestone lake, Manitoba, Canada, *Miner. Eng.*, 8(1995), No. 1-2, p. 159.
[24] S. Wang, M. Chen, Y.F. Guo, T. Jiang, and B.J. Zhao, Reduction and smelting of vanadium titanomagnetite metallized pellets, *JOM*, 71(2019), No. 3, p. 1144.
[25] L.S. Zhao, L.N. Wang, D.S. Chen, H.X. Zhao, Y.H. Liu, and T. Qi, Behaviors of vanadium and chromium in coal-based direct reduction of high-chromium vanadium-bearing titanomagnetite concentrates followed by magnetic separation, *Trans. Nonferrous Met. Soc. China*, 25(2015), No. 4, p. 1325.
[26] T. Hu, X.W. Lv, C.G. Bai, Z.G. Lun, and G.B. Qiu, Reduction behavior of panzhihua titanomagnetite concentrates with coal, *Metall. Mater. Trans. B*, 44(2013), No. 2, p. 252.
[27] T. Jiang, J. Xu, S.F. Guan, and X.X. Xue, Study on coal-based direct reduction of high-chromium vanadium–titanium magnetite, *J. Northeast. Univ.*, 36(2015), No. 1, p. 77.
[28] M.S. Jena, H.K. Tripathy, J.K. Mohanty, J.N. Mohanty, S.K. Das, and P.S.R. Reddy, Roasting followed by magnetic separation: A process for beneficiation of titano-magnetite ore, *Sep. Sci. Technol.*, 50(2015), No. 8, p. 1221.
[29] K. Ishizaki, K. Nagata, and T. Hayashi, Production of pig iron from magnetite ore–coal composite pellets by microwave heating, *ISIJ Int.*, 46(2006), No. 10, p. 1403.
[30] P. Ramdohr, *The Ore Minerals and Their Intergrowths*, Elsevier, Netherlands, 1969.
[31] S.H. Guo, W. Li, J.H. Peng, H. Niu, M.Y. Huang, L.B. Zhang, S.M. Zhang, and M. Huang, Microwave-absorbing characteristics of mixtures of different carbonaceous reducing agents and oxidized ilmenite, *Int. J. Miner. Process.*, 93(2009), No. 3-4, p. 289.
[32] C.A. Pickles, J. Mouris, and R.M. Hutcheon, High-temperature dielectric properties of goethite from 400 to 3000 MHz, *J. Mater. Res.*, 20(2005), No. 1, p. 18.
[33] K. Kawahira, Y. Saito, N. Yoshikawa, H. Todoroki, and S. Taniguchi, Penetration depth of microwave into the mixture of goethite with graphite estimated by permittivity and conductivity, *Metall. Mater. Trans. B*, 45(2014), No. 1, p. 212.
[34] Y. Saito, K. Kawahira, N. Yoshikawa, H. Todoroki, and S. Taniguchi, Dehydration behavior of goethite blended with graphite by microwave heating, *ISIJ Int.*, 51(2011), No. 6, p. 878.